Published in final edited form as:
Fly (Austin). 2007 ; 1(3): 146–152.

reduced ocelli Encodes the Leucine Rich Repeat Protein *Pray For Elves* in *Drosophila melanogaster*

Jason C. Caldwell, **Sarah K. Fineberg**, and **Daniel F. Eberl***
Department of Biological Sciences; University of Iowa; Iowa City, Iowa USA

Abstract

The ocelli are three simple photoreceptors on the vertex of the fruit fly head. We sought to identify the gene encoded by the classical ocellar mutant, *reduced ocelli* (*rdo)*. Deficiency and inversion breakpoint mapping and P-element induced male recombination analyses were performed and *Pray For Elves* (*PFE*; CG15151; Fbgn0032661) emerged as a promising candidate for the *rdo* phenotype. The *PFE* locus maps to polytene region 36E on chromosome 2L between *elfless* (Fbgn0032660) and *Arrestin 1* (Fbgn0000120). FlyBase annotation predicts that *PFE* encodes a serine/threonine kinase, yet protein prediction programs revealed no kinase domain. These analyses suggest that *PFE* simply encodes a leucine rich repeat molecule of unknown function, but presumably functions in nervous system protein-protein interaction. Two classical spontaneous alleles of *rdo*, rdo^1 and rdo^2, were characterized and the underlying mutations result from a small deletion spanning exon 1/intron 1 and a *B104/roo* insertion into the 3′UTR of *PFE*, respectively. Transposase-mediated excisions of several P-elements inserted into the *PFE* locus revert the *rdo* phenotype and a full-length *PFE* cDNA is sufficient to rescue *rdo*. A Gal4 enhancer trap reveals a broad adult neural expression pattern for *PFE*. Our identification and initial characterization of the *rdo* locus will contribute to the understanding of neurogenesis and neural development in the simple photoreceptors of the Drosophila visual system.

Keywords

Drosophila; ocelli; visual system; *Pray For Elves*; Leucine Rich Repeat

INTRODUCTION

The Drosophila adult visual system is composed of the two bilateral compound eyes and three triangularly arrayed simple eyes, the ocelli (Fig. 1A). The ocelli are located on the vertex of the fly head, one medial and two more posterior and lateral. The compound eyes and the ocelli derive from third instar larval eye-antennal imaginal discs (Fig. 1B). The two lateral ocelli each derive from a single disc while the medial ocellus arises from the fusion of both discs after puparium formation. Each ocellus possesses a dome-like corneal lens, ~40 μm in diameter, that lies above a thin corneagenous cell layer and 75–95 photoreceptor cells.[1,2] In Drosophila, six rhodopsins, Rh1-6, have been identified;[3-11] Rh2 is specific to the ocellar photoreceptors and confers violet sensitivity.[7,12,13] A layer of pigment cells surrounds the cluster of photoreceptor cells and each individual photoreceptor cell contains a single rhabdomere and pigment granules between the end of the rhabdomere and the nucleus. Photoreceptor cells are joined by belt desmosomes near the pigment granule layer. Photoreceptor cell axons, with associated glial cells, are found proximal to the photoreceptor cell nucleus.[12,14] The axons of

*Correspondence to: Daniel F. Eberl; Department of Biological Sciences; The University of Iowa; Iowa City, Iowa 52242-1324 USA; Tel.: 319.335.1323; Fax: 319.335.1069; Email: daniel-eberl@uiowa.edu.

the photorecptor cells project to their corresponding ocellar ganglion and four giant ocellar interneurons from each ganglion project into the brain via the ocellar nerve.

Compared to the wealth of knowledge pertaining to visual transduction in the compound eyes relatively little is known about the function of the ocelli. Once thought to be important in the generation of endogenous rhythms, the ocelli, and indeed the compound eyes, are neither essential nor necessary for effectively wild-type circadian activity even though a major clock protein, PERIOD, is expressed in the photoreceptor cells of these structures.[15] Indeed, *no ocelli*, *ocelliless* and *reduced ocelli* mutants all have effectively wild-type circadian locomotor rhythms.[16] The ocelli are, however, involved in simple visual guidance and modulation of sensitivity of the compound eyes during phototaxis.[17,18] In this work, a combination of molecular aberration breakpoint and P-element-mediated mapping, phenotype reversion and rescue, and molecular characterization of two extant *rdo* alleles were performed to demonstrate that leucine rich repeat protein *PFE* is encoded by the classical mutant *reduced ocelli* (*rdo*). *Pray For Elves* (*PFE*) was named by Suzanna Lewis to voice her growing frustration and feelings of isolation during the FlyBase release 3 genome annotation. She prayed for magic elves to help her finish her work (FBrf0151677).

RESULTS

Bioinformatics

Flies trans-heterozygous for the *Df(2L)B11* and *Df(2L)TW119* deficiencies and flies trans-heterozygous for *Df(2L)T317* and *In(2L)noc*^{2} exhibit *reduced ocelli* defects. Based on the estimated breakpoints of the overlapping deficiencies and the reported polytene chromosome breakpoint of *In(2L)noc*^{2} (Fig. 1C), *PFE* was investigated as a candidate for the *reduced ocelli* (*rdo*) phenotype. The *PFE* genomic region is 57,843 basepairs due to the presence of 39,054 basepair-spanning 5′ UTR and the 10,767 basepair intron between exons 1 and 2 (Fig. 1D and E); no additional annotated genes are predicted within these large exons. Three non-coding exons are interspersed within the large 5′UTR and these total a mere 694 basepairs. Twelve coding exons are predicted for *PFE* and from the first ATG-containing exon to the predicted translation stop site, the *PFE* transcript is 2,226 basepairs; an 856 basepair 3′UTR is also predicted (Fig. 1E). A full-length, 3,792 basepair *PFE* cDNA clone, complete with 3′ and 5′ UTRs (Accession# BT004502; from the Berkeley Drosophila Genome Project Head cDNA Library clone #GH07373) was used for these analyses and the accuracy of the clone was first verified by sequencing.

PFE is predicted to encode a 741 amino acid protein with a signal peptide (amino acids 1–17), a leucine rich repeat (LRR) region (amino acids 105–416) and a single transmembrane domain (integral to the membrane amino acids 506–528) and regions of low complexity in the C-terminal end beyond the transmembrane region (Fig. 1F). PFE is predicted to localize to the plasma membrane and the N-terminal LRR region is predicted to be extracellular. Leucine rich repeats are 20-29 basepair motifs predicted to be involved in a great diversity of biological functions that require protein-protein interaction.[19] The core LRR motif is LxxLxL,[20] where x is any amino acid; PFE is predicted to encode 10 such repeats. There are no additional domains predicted for PFE and pairwise alignment of PFE with all LRR containing proteins encoded in the *D. melanogaster* genome[21,22] reveals only 20–30% identity almost exclusively in the LRR region (data not shown). *PFE* therefore seems to simply encode an LRR protein, despite predictions inferred from genome annotation that this molecule has a serine/threonine kinase function.[21]

BLAST analysis of PFE revealed four similar molecules with no predicted function, from *D. pseudoobscura* (GA13532, 85% identity), *A. gambiae* (Q7Q1I6, ENSANGP00000014371, 51% identity), *A. aegyptus* (EAT36134; 49% identity) and *T. castaneum* (XP_969045; 36%

identity). These molecules have the same general protein architecture as *PFE* although the number of LRRs varies slightly and the *A. gambiae* ortholog has no predicted signal peptide (Table 1). tBLASTn analysis identified PFE orthologs in all of the sequenced[23] Drosophilid species (Table 1). A neighbor-joining tree was generated with the orthologs listed in Table 1, and as expected, the Drosophilid members are most closely related (Fig. 2). Very little is known about the function of the ocelli in these insect species and interestingly, unlike *D. melanogaster*, *A. gambiae*, *A. aegyptus* and *T. castaneum* all possess ocelli at larval stages, but not as adults. Indeed, in the yellow fever mosquito, *A. aegyptus*, the larvae possess a group of four lateral ocelli on each side of the head capsule.[24] And the rhodopsin molecules in these simple eyes have a peak absorbance at a wavelength of 515 nm and a maximal spectral sensitivity at 520 nm (green);[25,26] in *D. melanogaster* ocelli the peak spectral sensitivities are at 350–370 nm (ultra-violet) and 445 nm (blue).[18]

P-element induced male recombination (PIMR) mapping of *rdo*

As mentioned previously, we had some evidence, based on breakpoint mapping to suggest that *rdo* encodes *PFE*. PIMR[27] on the P-element P{SuporP}KG02815 (henceforth KG02815) inserted to the left of the 5′UTR of *PFE* (Fig. 1D) was performed in order to map rdo^2 relative to the P-element insertion. Recombinants were analyzed in trans with *Df(2L)TW119* to map the rdo^2 mutation relative to the KG02815 P-element cross-over event. In trans with *Df(2L)TW119*, four Sp^+ *pr* class recombinants were all rdo^- while in the *Sp* pr^+ class, one recombinant was rdo^+ and another, designated KG02815-D, was rdo^-. Two overall conclusions can be made from analysis of these male recombinant lines: 1) rdo^2 maps to the right of P-element KG02815, as expected if *rdo* encodes *PFE*, and 2) the *rdo* phenotype in KG02815-D is likely the result of a flanking deletion into the 5′UTR of *PFE* during P-element mobilization.[28] However, further molecular analyses of this line have not been performed.

P-element insertions at *PFE*

Three P-element inserts into different locations along the ~40 kilobase *PFE* 5′UTR (pre-ATG) (Fig. 1D) were investigated for these analyses including: P{SuporP}KG03741, P{SuporP}KG05889 and the Gal4 enhancer trap line P{GawB}8-156 (henceforth, KG03741, KG05889 and *PFE*-Gal4, respectively).[29,30] The *rdo* phenotype resulting from insertion of the KG elements is somewhat unexpected since the transposons do not insert into the predicted non-coding exons. The defects seen in these lines are likely due to the *suppressor of Hairy wing* [*su(Hw)*] chromatin insulator sites flanking the mini-white gene on the P-element. The *su(Hw)* insulators and the propensity for P-elements to insert at the 5′ end of genes, often results in altered levels of gene expression by disruption of the typical enhancer/promoter dynamic.[30-32] These three P-element lines are all rdo^-; the KG05889 insertion chromosome is homozygous lethal and therefore was tested for *reduced ocelli* in trans with *Df(2L)TW119*. Mobilizations of KG03741, KG05889 and *PFE*-Gal4 were also performed using standard transposase mediated techniques and excisions of these elements reverted the *rdo* phenotype (data not shown).

Extant alleles rdo^1 and rdo^2 disrupt *PFE*

Two extant spontaneous *rdo* alleles, rdo^1 and rdo^2,[33] were characterized for this study. It has been previously shown that *rdo* mutations result in variable reductions in size of the ocellar lens[2], although rdo^1 is generally more penetrant than rdo^2 (personal observations), and the number of ocellar receptor cells is reduced by about half in *rdo* homozygotes or *rdo*/*Df(2L)TW119* heterozygotes.[2]

We sequenced the *PFE* coding regions of these alleles to identify the mutations. rdo^1 is a small 158 basepair deletion of a region extending from exon 1 into intron 1 (Fig. 3A and B). RT-PCR analysis reveals that no *PFE* transcript is detectable in rdo^1 mutants (Fig. 3C). The 3′UTR

of *rdo*^{2} consistently failed to PCR amplify and iPCR analysis of *rdo*^{2} indicated that a *B104*/*roo* retrotransposon[34] is inserted into the 3′UTR of *PFE*; a 6 bp insertion site duplication (GGTGTT) is also evident (Fig. 3E). RT-PCR analysis of *rdo*^{2} was performed and *PFE* transcript is detectable in these mutants (Fig. 3D). To determine if the level of *PFE* transcript is reduced in *rdo*^{2} quantitative real time PCR was performed. Total mRNA pools were isolated from adults and *PFE* was weakly expressed in both *w*^{1118} and *rdo*^{2}; an approximate 2-fold difference in transcript copy number is evident in *rdo*^{2} (no significant difference, ANOVA p = 0.1686, Table 2). Since *rdo*^{2} is a *B104/roo* insertion into the 3′UTR it is possible that mRNA stability is variable—consistent with the weaker penetrance of this allele—and, as a result, a significant difference is masked. It is therefore possible that the level of PFE protein is reduced, but in the absence of a PFE antibody this possibility cannot be presently addressed. Alternatively, the effects on transcript level may not be uniform throughout the adult tissues. Finally, we PCR amplified the *PFE* coding regions in *In(2L)noc*^{2}*/Df(2L)T317* flies but were unable to find the breakpoints of the inversion, suggesting that the breakpoint of *In(2L)noc*^{2} is likely to be in the 40 Kb 5′UTR of *PFE*.

The *PFE*-Gal4 enhancer trap driving UAS-*PFE* rescues *rdo*

A *PFE*-Gal4 enhancer trap insertion (P{GawB}8-156) into noncoding exon A (Fig. 1D) of *PFE* causes the *rdo* phenotype. A full-length *PFE* cDNA was cloned into the pUAST vector (UAS-*PFE)* and, in *w*; *PFE*-Gal4; UAS-*PFE*/*TM3* flies, *rdo* appears to be fully rescued to wild-type, as determined by observing the ocelli under a dissecting scope (n = 30) and with SEM (n = 3). These data indicate that UAS-*PFE* is sufficient to rescue, and is encoded by, *rdo* (Fig. 4). Likewise, with the ubiquitous driver *spaghetti-squash*-Gal4[35], UAS-*PFE* is also sufficient to rescue *rdo* in *Df(2L)TW119*/*Df(2L)B11* flies (data not shown). Heterozygous *PFE*-Gal4 (*rdo*$^+$) driven expression of UAS-nls-GFP (nls; nuclear localization signal) is evident in all third instar larval imaginal discs in proneural cluster cells (Fig. 5A; A. Christiansen, personal communication) and this expression pattern is identical to previously reported in situ data using a full length *PFE* cDNA probe.[36] In adults, GFP expression is evident in much of the nervous system including, but not limited to, the femoral chordotonal organ neurons and bristle neurons, the wing vein campaniform sensilla and wing margin bristle neurons, the compound eye facets, the lateral and medial ocelli and the olfactory chemoreceptors of the third antennal segment (Fig. 6). One caveat from these data is that the enhancer trap may not respond to any negative regulatory elements. In other words, in adults, *PFE* expression may be limited to the ocelli—consistent with the mutant phenotype—but, in the absence of adequate silencers, expression in the nervous system is robust. On the other hand, *PFE* may be functionally redundant in all tissues except the ocelli and therefore *rdo* only manifests in the ocelli.

CONCLUSIONS

We have presented several pieces of evidence that indicate *PFE* is encoded by *rdo*. Initially our genetic mapping with overlapping deficiencies and other chromosomal aberrations refined the *rdo* region. P-element induced male recombination indicated that *rdo*^{2} was to the right of the KG02815 P-element insert. Furthermore, several P-elements inserted into the *PFE* 5′UTR resulted in *rdo* and this phenotype was reverted when the elements were precisely excised. A UAS-*PFE* construct, when driven by a *PFE*-specific Gal4 enhancer trap, reverts the *rdo* phenotype, indicating that *PFE* is sufficient to rescue *rdo*. We also identified the mutations in *PFE* in two extant alleles of *rdo*. *rdo*^{1} results from a small deletion and lacks detectable *PFE* transcript and is therefore a null allele. *rdo*^{2} is a *B104*/*roo* retrotransposon insertion into the 3′ UTR of *PFE* and transcripts are detectable by real time PCR and not significantly reduced compared to controls.

As demonstrated by Gal4-enhancer trap analysis and in situ hybridization with a full-length *PFE* cDNA, a broad neural expression pattern is evident for *PFE* although the only observed mutant phenotype is reduced ocelli; the most parsimonious explanation for this difference is that *PFE* may simply be expressed in non-essential regions. On the other hand, these data suggest that *PFE* mutants may not exhibit a more severe sensory phenotype due to functional redun-dancy with other LRR proteins. Furthermore, *PFE* is predicted to be post-transcriptionally regulated by microRNAs and this regulation may be spatially active in all tissues other than the ocelli. *PFE* may also be translationally or post-translationally regulated and, as a result, the protein, or putative active version of the protein, may only be present in the ocelli. Perhaps a more enticing explanation is that additional phenotypes have not been uncovered due to the purely morphological approach to our experimental design; in our laboratory strains, *PFE* may be involved in a presently unidentified, non-essential sensory process. *rdo* mutants have normal sound-evoked potentials in the antennal nerve (D. Eberl, unpublished). No electroretinograms have been performed on *rdo*. Nevertheless, we were able to definitively attribute *rdo* to *PFE* and future studies will focus on investigating the role of this LRR protein in ocellar system development. We are particularly interested in determining if *PFE* is redundant to other LRR molecules and the role of the LRR motif in protein-protein interactions necessary for proper formation of the ocelli.

EXPERIMENTAL PROCEDURES

Animals

Genetic strains of *Drosophila melanogaster* included seven mutant strains, four P-element lines and one normal control. The control strain was the w^{1118} (FBal0018186) strain; transformants were generated in the w^{1118} background. Stock of spontaneous *reduced ocelli* alleles of the genotypes rdo^{1} (FBal0014506) and rdo^{2} *pr* (FBal0014507) were obtained from the Bloomington Stock Center. Chromosomal deficiencies used to map *rdo* were *Df(2L) TW119*, *cn bw/CyO*[37] (Bloomington; FBab0001642), *Df(2L)B11*, *nub bpr/CyO* (Bob Hardy, UCSD; FBab0040370), $In(2L)noc^{2}/CyO$[38] (John Roote, Cambridge; FBab0004671), and *Df (2L)T317*, *b pr cn sca/CyO*[39] (Bloomington; FBab0001563). The *w*; *TW12*, *Tft pr*/*CyO pr* (Bloomington; FBab0001643) strain was used for PIMR. P-element lines KG03741 (FBst0013966), KG05889 (FBst0014132) and KG02815 (FBst0012989) were isolated from the Berkeley Drosophila Genome Project KG Enhancer Trap screen (http://www.fruitfly.org/p_disrupt/) and obtained from the Bloomington Stock Center. The 8-156 *(PFE*-Gal4) enhancer trap line was a generous gift from Audrey Christiansen and was originally obtained from the private enhancer trap collection in the Heberlein lab.

Bioinformatics

Protein architectures for PFE and orthologs were analyzed using the following servers and default parameters: SignalP 3.0 server (http://www.cbs.dtu.dk/services/SignalP/), TMHMM server (http://www.cbs.dtu.dk/services/TMHMM/) and SMART (http://smart.embl-heidelberg.de/). Subcellular localization of PFE was predicted with PSORT II (http://psort.hgc.jp). BLAST analyses were performed with the predicted full-length PFE protein sequence as input. *D. pseudoobscura*, mosquito and red flour beetle PFE orthologs were identified by BLASTp (http://www.ncbi.nlm.nih.gov/BLAST/) with no filter for low complexity. PFE orthologs in other Drosophilid species were identified with tBLASTn at DroSpeGe (http://insects.eugenes.org/species/blast/). DNA sequences from the DroSpeGe search output were six-frame translated at the BCM Search Launcher (http://searchlauncher.bcm.tmc.edu/) and aligned with PFE with BLAST 2 Sequences (http://www.ncbi.nlm.nih.gov/blast/bl2seq/wblast2.cgi) to determine % identity. Sequences were aligned with ClustalW (with slow/accurate parameters) at http://align.genome.jp/ to generate an unrooted Neighbor-Joining Tree.

PIMR

Prior to performing PIMR, *rdo*^{2} was crossed into a background with several 2nd chromosome markers and a source of transposase—the resulting strain had the following genotype: w^+; *Sp rdo*^{2} *pr rl cn*/*CyO*; *Dr*,Δ*2-3*/*TM6, Ubx*. Females of this strain were crossed to males of the P-element carrying strain, *w*/Y; KG02815. w^+/Y; *Sp rdo*^{2} *pr rl cn*/KG02815; *Dr*, Δ*2-3*/+ males were collected and crossed to *w*; *TW12 Tft pr*/*CyO pr* females. *Sp*$^+$ *pr* or *Sp pr*$^+$ recombinants were collected over *CyO* or the *Tft* chromosome.

Reverse transcriptase PCR and real time PCR

For reverse transcriptase PCR, total RNA was isolated from tissues using the RNeasy mini kit (Qiagen 74104) with DNaseI treatment (Qiagen 79254) per kit instructions. For first strand synthesis, 5 μl of isolated total RNA was added to 1.25 μl poly-d(T)$_{12-18}$ primer (Amersham 27-7858-02), 1 μl dNTPs and 1.25 μl DEPC-H_2O and this mixture was heated to 65°C for 5 minutes and then cooled on ice for 5 minutes. Ten μl of 5x reaction buffer (250 μM Tris-HCl pH 8.3, 375 μM KCl, 15 μM $MgCl_2$; Invitrogen 18064-022) and 5 μl 0.1M DTT (Invitrogen 18064-022) and 2.5 μl of Recombinant RNasin ribonuclease inhibitor (Promega N251A) were added and the mixture was heated to 42°C for 2 minutes. Then reverse transcriptase (Invitrogen 18064-022) or DEPC treated water was added for Rt+ or Rt-, respectively, and then incubated for 42°C for 50 minutes. The first strand synthesis reaction was inactivated at 70°C for 15 minutes. The cDNA was then used in a standard PCR reaction with *DmCa1D* (FBgn0001991) control primers DmCa1DF [5′-CAACCGGATGTGAAGTGCG-3′] and DmCa1DR [5′-CTT GGCACTTCGCCTGAAGG-3′] (data not shown), as well as, *PFE* primers directed against exons 1 and 3, PFE-RT1F [5′-GCTCTTCAAGTGGCTCCTG-3′] and PFE-RT3R [5′-GAAACGTTGAACTGGCCATG-3′] primers and the program [{95°C/30 s, 54Δ7°C/30 s, 72° C/30 s} × 30; {72°C/5 m} × 1].

For real time PCR, first strand synthesis was performed on isolated total RNA using the Superscript III First Strand Synthesis System (Invitrogen 18080-051) and oligo(dT)$_{20}$ primer per kit instructions. Real time PCR was carried out with isolated cDNAs and the SYBR Green PCR Master Mix (Applied Biosystems 4309155) with *Gapdh2* control primers Gapdh2-f [5′-AGCGCTGGTGCCGAATAC-3′] and Gapdh2-r [5′-AGTGAGTGGATGCCTTGTCGAT-3′] and *PFE* primers (described in reverse transcriptase section above). To control for pipetting errors, cDNAs from a biological sample were amplified in triplicate for both control and *PFE* primers; three biological samples per strain type were analyzed. NoRT controls for *Gapdh2* and *PFE* primer sets were also included in the real time PCR reaction for each biological sample; no template controls were also performed for both primer sets. Real time PCR was performed using the following cycling conditions: [{95°C/10 m} × 1; {95°C/15 s, 60°C/1 m} × 40] and a single dissociation protocol {60°C + 35°C/20 minutes}. In the dissociation step, a single peak was obtained for *Gapdh2* and *PFE* primers indicating only a single, specific product was amplified.

Inverse PCR

30 flies were collected and placed on ice briefly. Flies were homogenized in 200 μl Buffer A {100 μM Tris-HCl, pH 7.5, 100 μM EDTA, 100 μM NaCl, 0.5% SDS}. Another 200 μl of Buffer A was added and tissues were homogenized again and placed at 65°C for 30 minutes. Eight hundred microliters of LiCl/KAc Solution {1 part 5 M KAc, 2 parts 6 M LiCl} were added and the sample was incubated on ice for 10 minutes. Tubes were centrifuged for 15 minutes at max speed. One milliliter of supernatant was removed to a new tube and 600 μl isopropanol were added. Tubes were centifuged for 15 minutes at max speed. The supernatant was discarded and washed with 70% EtOH. Pellets were resuspsended in 150 μl TE. 10 μl of the sample in TE with 2.5 μl Sau3AI with 2.5 μl BSA, 2 μl 100 μg/ml RNAseA, 2.5 μl Sau3AI buffer and 5.5 μl H_2O was digested for 2.5 hours at 37°C and heat inactivated 20 minutes at

65°C. 10 μl of the Digested Genomic DNA was ligated in a large volume (12 μl 10X ligation buffer, 1 μl 400,000 U/μl Ligase and 97 μl H_2O) overnight at 4°C. 360 μl QG buffer from QIAquick Gel Extraction Kit (Qiagen 28704) and 120 μl isopropanol was added. Contents were added to gel extraction column and centrifuged at 13,000 rpm for 1 minute. The flow through was discarded and 750 μl PE buffer from QIAquick Gel Extraction Kit (Qiagen 28704) was added to the column for a 2 minute incubation; the tube was centrifuged briefly and the flow through discarded, followed by a 1 minute spin to dry column. Ligated products were eluted with 50 μl EB from QIAquick Gel Extraction Kit (Qiagen 28704) and a 1 minute spin. PCR was performed with 10 μl of template, 1 μl of Forward primer, 1 μl Reverse Primer, 1 μl dNTPs (50X), 5 μl 10X buffer, 1.5 μl $MgCl_2$, 0.5 μl Taq and 30 μl H_2O. The left side of the break was determined using PFE-iLeft-inF [5′-GTACACACGATTCATTTCGACAC-3′] and PFE-iLeft-inR [5′-GTGAAACACTGGTAAAGTTCG-3′] and the right side of the break was determined with PFE-iRight-outF [5′-GGTAAGGTCTTCTTGCGAGC-3′] and PFE-iRight-outR [5′-GAACTAGCATGTAAGGCATGTC-3′].

Rescue construct

A full-length (including 5′ and 3′ UTRs) cDNA clone of *PFE* was PCR amplified from the BDGP EST clone GH07373, using primers POT2F [5′-AATGCAGGTTAACCTGGCTTATCG-3′] and POT2R [5′-AACGCGGCTACAATTAATACATAACC-3′], and the program [{95°C/30 s, 56.5°C/30 s, 72°C/2 m} × 30; {72°C/10 m} × 1]. The PCR product was cloned into TOPO-XL and confirmed by sequencing. Full-length PFE was directionally subcloned into pUAST[40] and injected by the Duke University Model System Genomics Facility.

Scanning electron microscopy

Heads were isolated and fixed in 2.5% gluteraldehyde for 24 hours at 4°C, postfixed in 1% OsO_4/Phosphate Buffer for 1 hour, dehydrated in an ethanol series, critical point dried and finally sputter coated with a layer of Gold/Palladium. Images were taken on a Hitachi S-4000.

Statistical analysis

Real time PCR data were analyzed by ANOVA using SAS version 6.12 (Sas Institute Inc., Cary, NC, USA).

ACKNOWLEDGEMENTS

We would like to thank Audrey Christiansen and the Bloomington Drosophila stock center for providing fly stocks, the Elena Sivan Loukianova and the UI Central Microscopy Research Facility for SEMs, Jill Pottratz for deficiency mapping and the Duke University Model Systems Genomics Facility for injection of the UAS-*PFE* construct.

FUNDING

Daniel F. Eberl: NIH grant DC04848

ABBREVIATIONS

rdo, reduced ocelli; PFE, Pray For Elves; LRR, leucine rich repeat; PIMR, P element induced male recombination.

Reference

1. García-Alonso L, Fetter RD, Goodman CS. Genetic analysis of Laminin A in Drosophila: Extracellular matrix containing laminin A is required for ocellar axon pathfinding. Development 1996;122:2611–21. [PubMed: 8787736]

2. Stark WS, Sapp R. Ultrastructure of the ocellar visual system in normal and mutant *Drosophila melanogaster*. J Neurogenetics 1989;5:127–53. [PubMed: 2500507]
3. Zuker CS, Montell C, Jones K, Laverty T, Rubin GM. A rhodopsin gene expressed in photoreceptor cell R7 of the Drosophila eye: Homologies with other signal-transducing molecules. J Neurosci 1987;7:1550–7. [PubMed: 2437266]
4. Zuker CS, Mismer D, Hardy R, Rubin GM. Ectopic expression of a minor Drosophila opsin in the major photoreceptor cell class: Distinguishing the role of primary receptor and cellular context. Cell 1988;53:475–82. [PubMed: 2966681]
5. Zuker CS, Cowman AF, Rubin GM. Isolation and structure of a rhodopsin gene from *D. melanogaster*. Cell 1985;40:851–8. [PubMed: 2580638]
6. O'Tousa JE, Baehr W, Martin RL, Hirsh J, Pak WL, Applebury ML. The Drosophila *ninaE* gene encodes an opsin. Cell 1985;40:839–50. [PubMed: 2985266]
7. Cowman AF, Zuker CS, Rubin GM. An opsin gene expressed in only one photoreceptor cell type of the Drosophila eye. Cell 1986;44:705–10. [PubMed: 2936466]
8. Montell C, Jones K, Zuker C, Rubin G. A second opsin gene expressed in the ultraviolet-sen-sisite R7 photoreceptor cells of *Drosophlia melanogaster*. J Neurosci 1987;7:1558–66. [PubMed: 2952772]
9. Papatsenko D, Sheng G, Desplan C. A new rhodopsin in R8 photoreceptors of Drosophila: Evidence for coordinate epxression with Rh3 in R7 cells. Development 1997;124:1665–73. [PubMed: 9165115]
10. Chou WH, Hall KJ, Wilson DB, Wideman CL, Townson SM, Chadwell LV, Britt SG. Identification of a novel Drosophila opsin reveals specific patterning of the R7 and R8 photoreceptor cells. Neuron 1996;17:1101–15. [PubMed: 8982159]
11. Huber A, Schulz S, Bentrop J, Groell C, Wolfrum U, Paulsen R. Molecular cloning of Drosophila Rh6 rhodopsin: The visual pigment of a subset of R8 photoreceptor cells. FEBS Lett 1997;406:6–10. [PubMed: 9109375]
12. Pollock JA, Benzer S. Transcript localization of four opsin genes in the three visual organs of Drosophila; RH2 is ocellus specific. Nature 1988;333:779–82. [PubMed: 2968518]
13. Mismer D, Michael WM, Laverty TR, Rubin GM. Analysis of the promoter of the Rh2 opsin gene in *Drosophila melanogaster*. Genetics 1988;120:173–80. [PubMed: 2975615]
14. Yoon CS, Hirosawa K, Suzuki E. Studies on the structure of ocellar photoreceptor cells of *Drosphila melanogaster* with special reference to subrhabdomeric cisternae. Cell Tisues Res 1996;284:77–85.
15. Ewer J, Frisch B, Hamblen-Coyle MJ, Rosbash M, Hall JC. Expression of the period clock gene within different cell types in the brain of Drosophila adults and mosaic analysis of these cells' influence on circadian behavioral rhythms. J Neurosci 1992;12:3321–49. [PubMed: 1382123]
16. Vosshall LB, Young MW. Circadian rhythms in Drosophila can be driven by period expression in a restricted group of central brain cells. Neuron 1995;15:345–60. [PubMed: 7646889]
17. Fischbach K, Reichert H. Interactions of visual subsystems in *Drosophila melanogaster*: A behavioural genetic analysis. Biol Behav 1978;2:305–17.
18. Hu KG, Stark WS. The roles of Drosophila ocelli and compound eyes in phototaxis. J Comp Physiol A 1980;135:85–95.
19. Kobe B, Kajava AV. The leucine-rich repeat as a protein recognition motif. Curr Opin Struct Biol 2001;11:725–32. [PubMed: 11751054]
20. Kajava AV, Kobe B. Assessment of the ability to model proteins with leucine-rich repeats in light of the lastest strutural information. Protein Sci 2002;11:1082–90. [PubMed: 11967365]
21. Grumbling G, Strelets V. The Flybase Consortium. FlyBase: Anatomical data, images and queries. Nucleic Acids Res 2006;34:D484–8. [PubMed: 16381917]
22. Hynes RO, Zhao Q. The evolution of cell adhesion. J Cell Biol 2000;150:F89–F95. [PubMed: 10908592]
23. Gilbert, D. DroSpeGe, a public database of Drosophila species genomes. http://insectseu- genesorg/DroSpeGe/2005http://insectseu- genesorg/DroSpeGe/2005
24. Brown P, White R. Rhodopsin of the larval mosquito. J Gen Physiol 1972;59:401–14. [PubMed: 5029551]
25. Seldin E, White R, Brown P. Spectral sensitivity of larval mosquito ocelli. J Gen Physiol 1972;59:415–20. [PubMed: 5029552]

26. White R. Analysis of the development of the compound eye in the mosquito, Aedes aegypti. J Exp Zool 1961;148:223–39. [PubMed: 14006559]
27. Chen B, Chu T, Harms E, Gergen JP, Strickland S. Mapping of Drosophila mutations using site-specific male recombination. Genetics 1998;149:157–63. [PubMed: 9584093]
28. Preston CR, Sved JA, Engels WR. Flanking duplications and deletions associated with P-inuced male recombination in Drosophila. Genetics 1996;144:1623–38. [PubMed: 8978050]
29. Bier E, Baessin H, Shepherd S, Lee K, McCall K, Barbel S, Ackerman L, Carretto R, Uemura T, Grell E, Jan LY, Jan YN. Searching for a pattern and mutation in the Drosophila with a P-*lacZ* vector. Genes Dev 1989;3:1273–87. [PubMed: 2558049]
30. Roseman RR, Johnson EA, Rodesch CK, Bjerke M, Nagoshi RN, Geyer PK. A P element containing *suppressor of Hairy-wing* binding regions has novel properties for mutagenesis in *Drosophila melanogaster*. Genetics 1995;141:1061–74. [PubMed: 8582613]
31. Bellen HJ. Ten years of enhancer detection: Lessons from the fly. Plant Cell 1999;11:2271–81. [PubMed: 10590157]
32. Liao GC, Rehm EJ, Rubin GM. Insertion site preferences of the *P* transposable element in *Drosophila melanogaster*. Proc Natl Acad Sci 2000;97:3347–51. [PubMed: 10716700]
33. Lindsley, D.; Zimm, GG. The Genome of *Drosophila melanogaster*. Academic Press; San Diego, California: 1992.
34. Scherer G, Tschudi C, Perera J, Delius H. *B104*, a new dispersed repeated gene family in *Drosophila melanogaster* and its analogies with retroviruses. J Mol Biol 1982;157:435–51. [PubMed: 6181263]
35. Kiehart DP, Galbraith CG, Edwards KA, Rickoll WL, Montague RA. Multiple forces contribute to cell sheet morphogenesis for dorsal closure in Drosophila. J Cell Biol 2000;149:471–90. [PubMed: 10769037]
36. Reeves N, Posakony JW. Genetic programs activated by proneural proteins in the developing Drosophila PNS. Dev Cell 2005;8:413–25. [PubMed: 15737936]
37. Wright TRF, Hodgetts RB, Sherald AF. The genetics of dopa decarboxylase in *Drosophila melanogaster*. I. Isolation and characterization of deficiencies of the structural locus and the a-methyldopa hypersensitive locus. Genetics 1976;84:267–85. [PubMed: 826447]
38. Ashburner M, Aaron C, Tsubota S. The genetics of a small autosomal region of *Drosophila melanogaster*, including the structural gene for alcohol dehydrogenase. V. Characterization of x-ray-induced *Adh* null mutations. Genetics 1981;102:421–35. [PubMed: 6816674]
39. Steward R, Nusslein-Volhard C. The genetics of the *Dorsal-Bicaudal-D* region of *Drosophila melanogaster*. Genetics 1986;113:665–78. [PubMed: 3089869]
40. Brand AH, Perrimon N. Targeted gene expression as a means of altering cell fates and generating dominant phenotypes. Development 1993;118:401–15. [PubMed: 8223268]

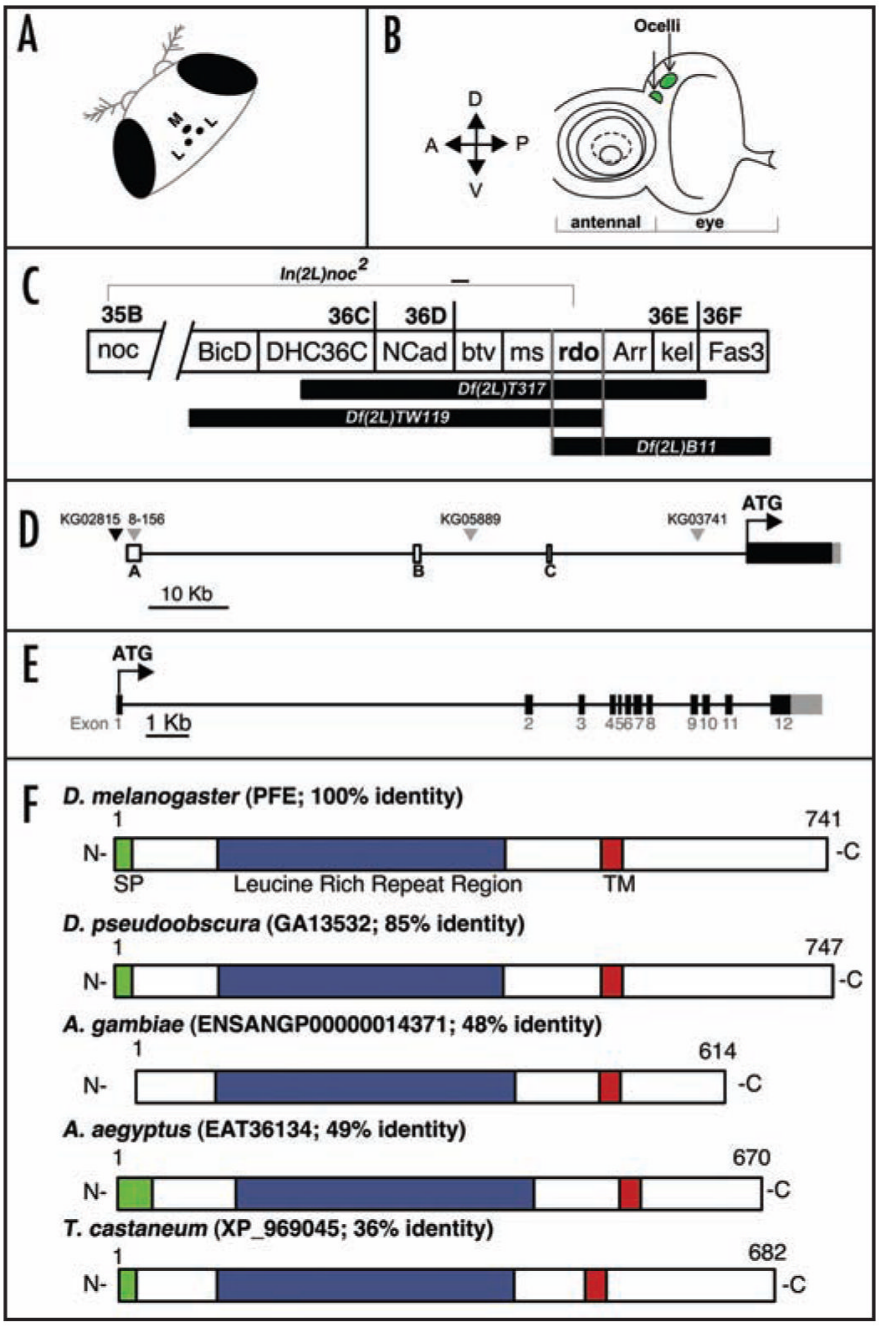

Figure 1.

The *rdo* genetic region and the *PFE* locus. (A) Cartoon of the medial ocellus (M) and the two lateral ocelli (L) situated on the vertex of the Drosophila head between the compound eyes. (B) Cartoon of the third instar larval eye-antennal disc with the ocellar primordia shaded green. (C) The reduced ocelli region was mapped to 36DE using overlapping deficiencies *Df(2L)TW119* and *Df(2L)B11* and overlapping aberrations *In(2L)noc*^{2} and *Df(2L)T317*. (D) The *PFE* genomic region consists of a large 5′UTR with three non-coding exons (unshaded boxes) a coding region (black box) and a 3′UTR (grey box). Three P-elements (grey triangles), 8-156 (also referred to in the text as *PFE-Gal4*), KG05889, KG03741, inserted in the 5′UTR, are *rdo*$^{-}$ and one P-element (black triangle), KG02815, is inserted upstream of *PFE* and is *rdo*$^{+}$.

(E) The *PFE* coding region consists of twelve exons (black boxes) and 11 introns (thin line); the 3′UTR in exon 12 is also shown (grey box). (F) Diagram of the PFE protein and four insect orthologs (% identity based on output from BLAST 2 sequences is indicated). SP; signal peptide, TM; Transmembrane domain.

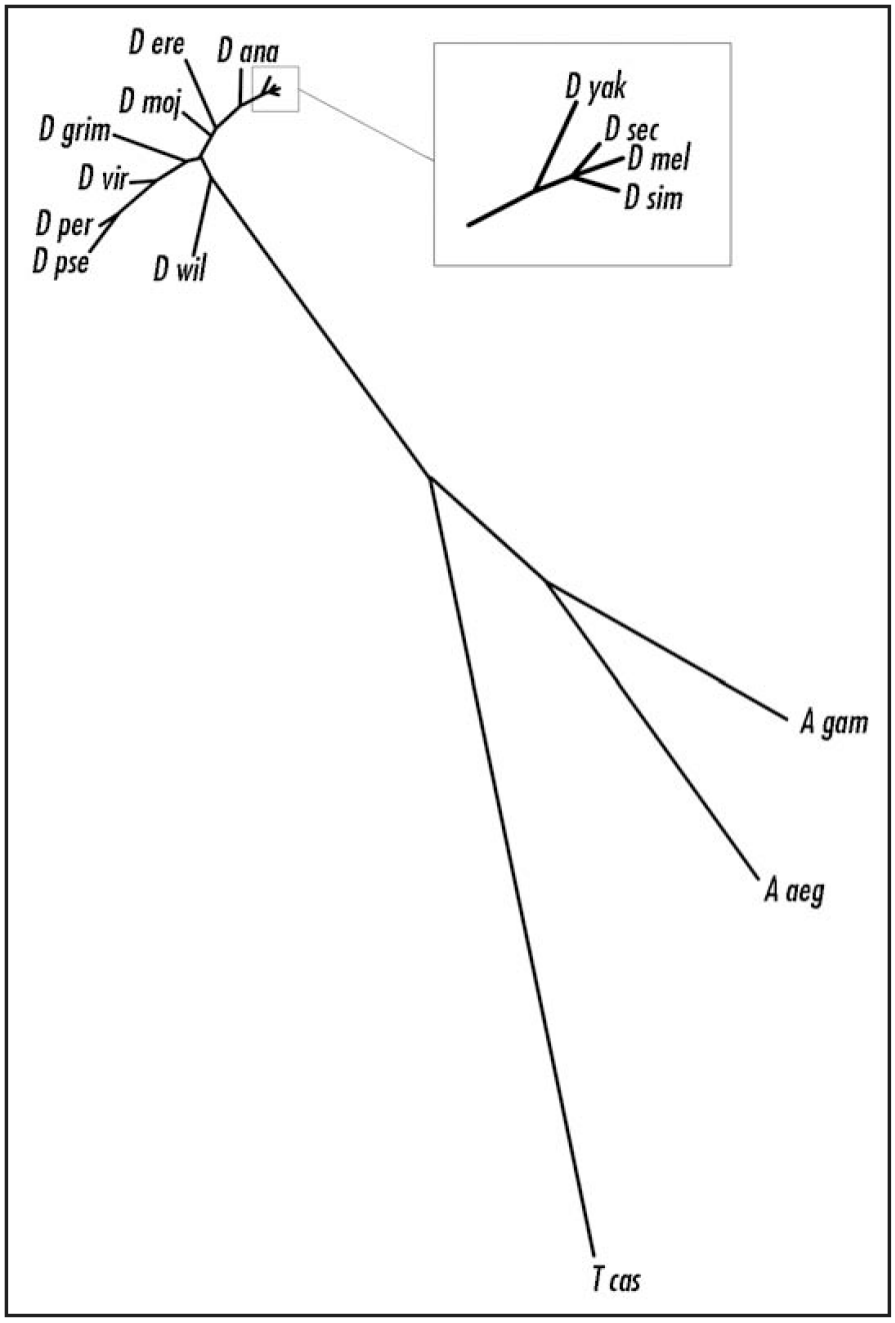

Figure 2.
Neighbor-joining tree of PFE orthologs. Comparison of the Drosophilid, mosquito and beetle PFE orthologs. See Experimental Procedures for construction of tree.

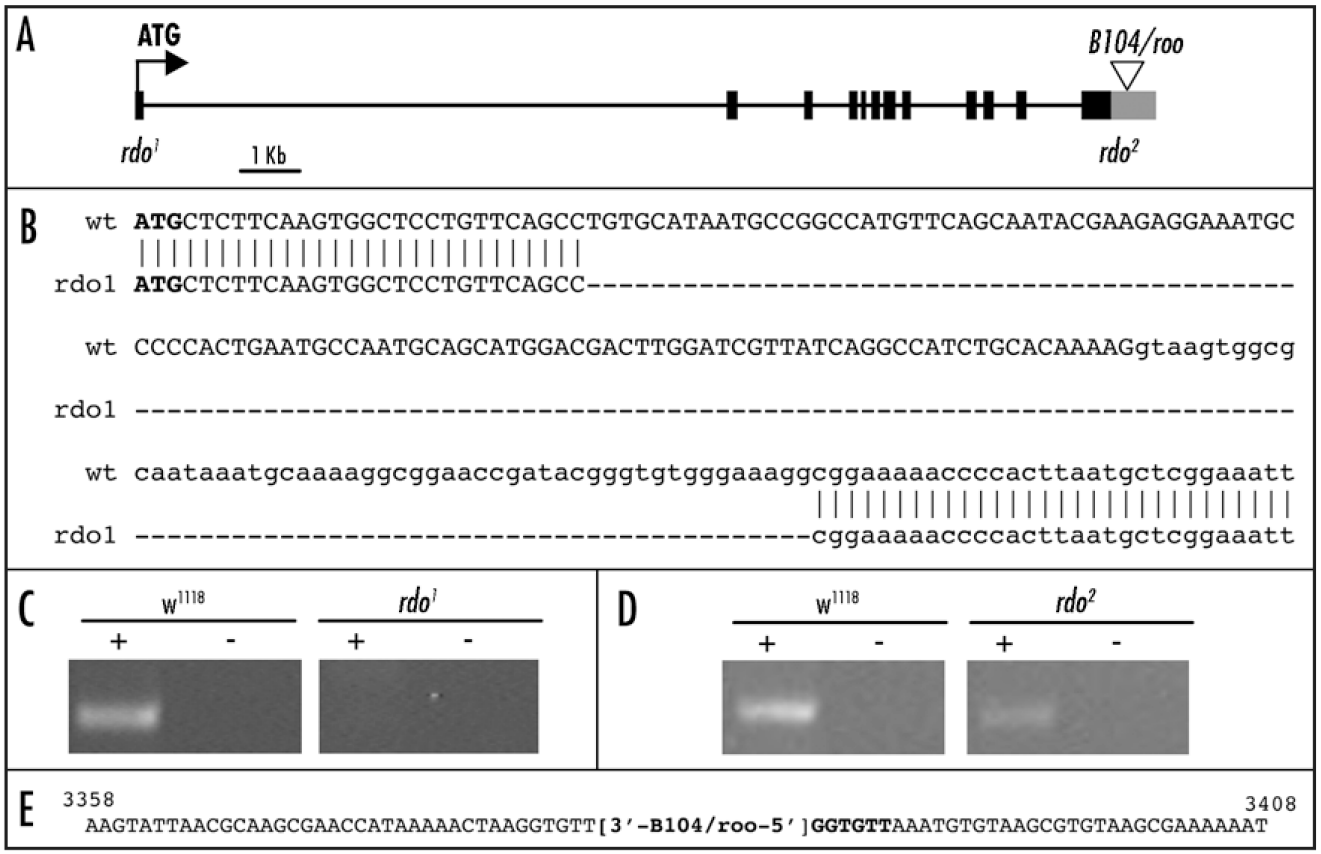

Figure 3.

Molecular identification of the *rdo*^{1} and *rdo*^{2} mutations. (A) Schematic of the *PFE* coding region (black boxes) and 3′UTR (grey box) shown with *B104/roo* insertion (unfilled triangle). (B) Sequence alignment of exon 1 (UPPERCASE) and a portion of intron 1 (lowercase) between wild-type and *rdo*^{1}. ATG start is indicated in bold, deleted region of *rdo*^{1} indicated by '-'. (C) RT-PCR analysis of *PFE* in control and *rdo*^{1} cDNA pools reveals no detectable *PFE* transcript in *rdo*^{1}. *DmCa1D* primers were used as a positive control (data not shown). (D) RT-PCR analysis of *PFE* in control and *rdo*^{2} cDNA pools indicates *PFE* transcript is detectable in both strains. *DmCa1D* primers were used as a positive control (data not shown). Real time PCR was conducted to analyze possible differences in *PFE* transcript level (see Table 2) (E) The *rdo*^{2} mutation is a *B104/roo* retrotransposon insertion (Accession #AY180917) into the 3′UTR of *PFE* with a flanking insertion site duplication (GGTGTT; bold). Numbering of wild-type sequence (normal font weight) is based on NCBI accession BT004502.

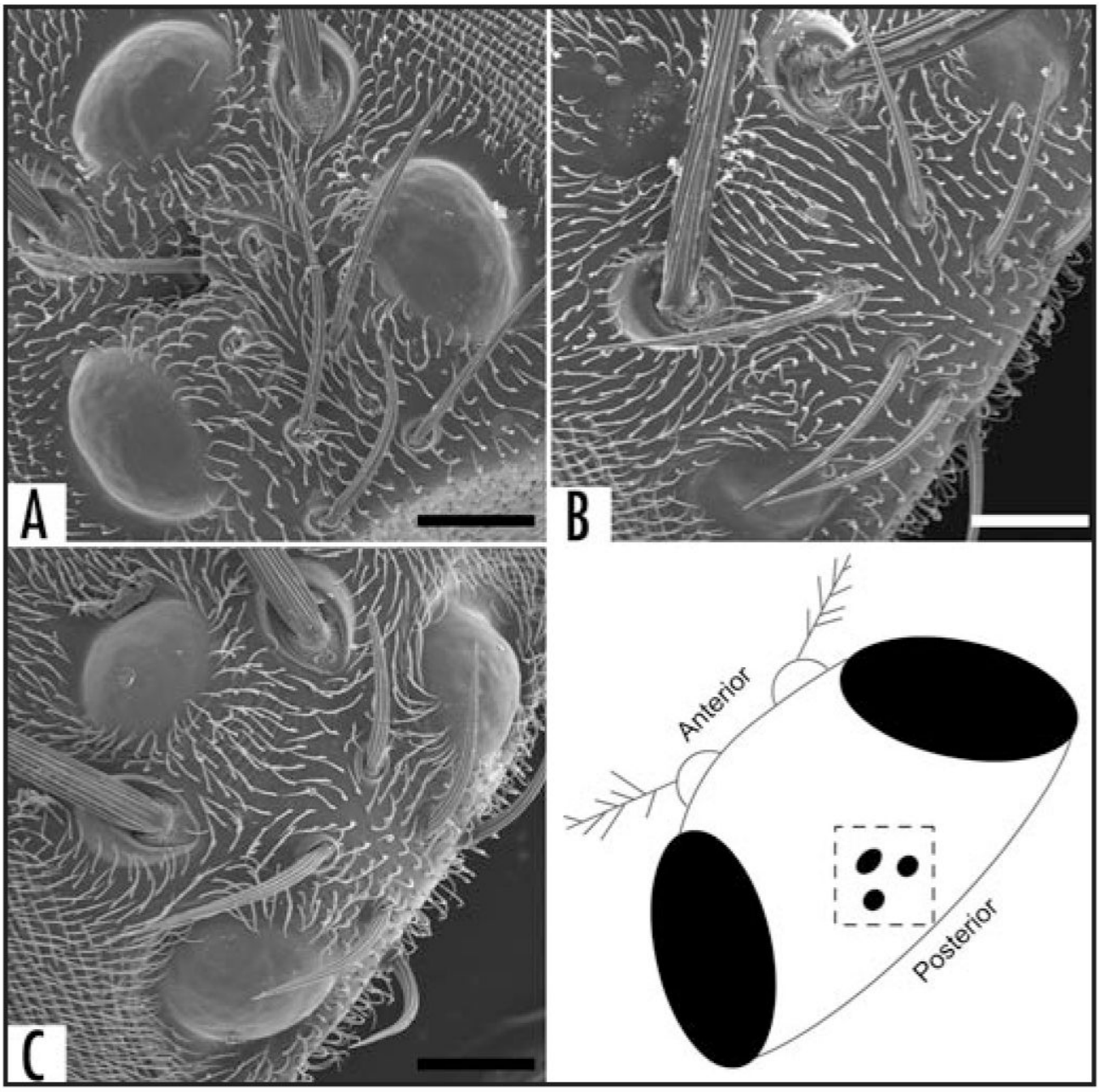

Figure 4.
Rescue of *rdo* with UAS-*PFE*. (A) w^{1118} control line with fully formed ocelli with normal scalloping evident on the ocellar lenses. (B) *w*; *PFE*-Gal4 (*rdo*) line with reduced ocellar lenses. The lateral lenses exhibit relatively normal scalloping while the medial ocellus exhibits corneal nipples (after Stark and Sapp, 1989). (C) *w*; *PFE*-Gal4; UAS-*PFE/TM3* flies have restored ocelli and scalloped lenses. Scale bars = 25 μm.

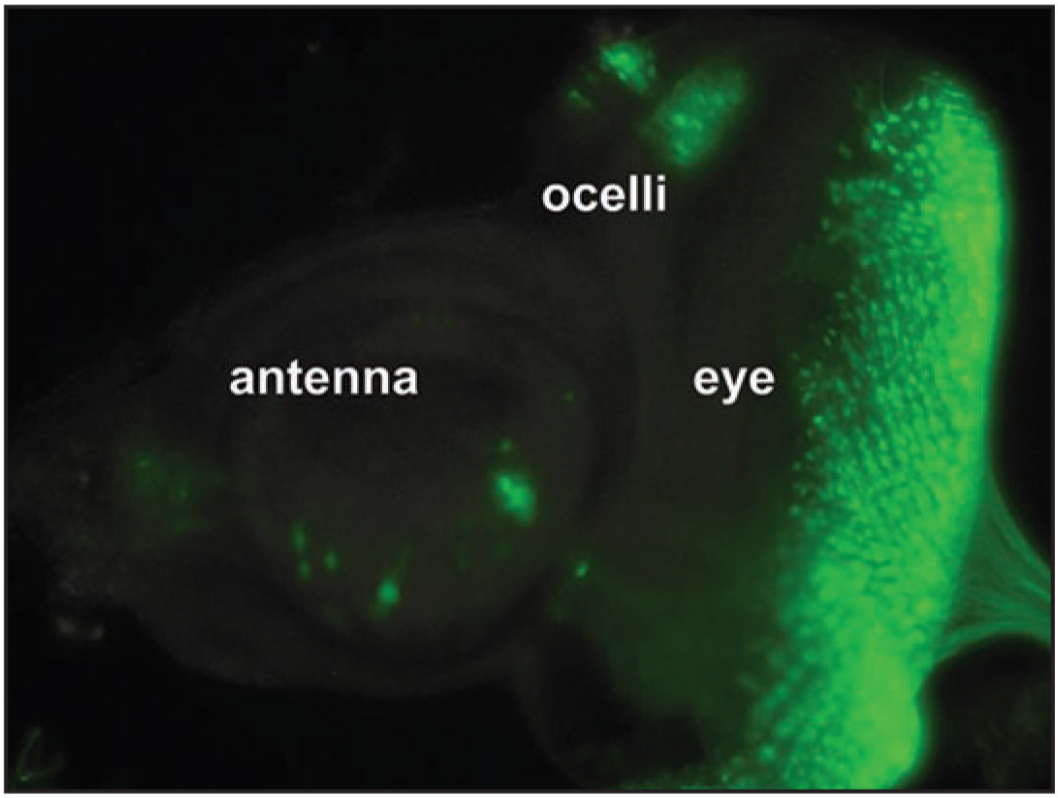

Figure 5.
The *PFE*-Gal4 enhancer trap drives expression of UAS-nls-GFP in the eye-antennal disc proneural cluster cells UAS-nls-GFP expression pattern was observed in *PFE*-Gal4 heterozygotes (rdo^{+}). GFP expression is evident in third instar larval eye-antennal imaginal disc proneural cluster cells including the ocellar, eye and antennal primordia. Photoshop was used to reduce the background over the entire image. The color range was selected to include only the intensely green areas and applied as a duplicated masking layer over the original image layer. The original image layer was then converted to black and white with a gradient map (black to white).

Figure 6.

PFE-Gal4 drives expression of UAS-GFP in the adult nervous system. UAS-GFP expression pattern was observed in *PFE*-Gal4 heterozygotes (rdo^{+}). (A) GFP expression is evident in the bristle neurons along the L1 wing vein margin and the campaniform sensilla of L2 wing vein. Wing vein L3 and the wing chordotonal organ cluster are not shown in this view but GFP expression is evident in these regions. (B) Expression in the bristle neurons of the tibia and tarsi is evident. (C) Expression in the adult head is evident in olfacatory chemoreceptors in the third antennal segment and palps, in the compound eyes and in the ocelli. An air bubble was airbrushed out of (C) using Photoshop.

Table 1

PFE orthologs

Species	%Identity	Span	#LRRs	ID
D. melanogaster	100	1–741	10	PFE/CG15151
D. simulans	98	1–741	9	wu050602
D. sechellia	98	1–741	10	br051028
D. yakuba	98	1–741	8	caf051213
D. erecta	95	4–741	8	ca051209
D. ananasse	76	1–741	7	caf051209
D. pseudoobscura	85	1–741	11	GA13532
D. persimilis	80	1–741	8	br051028
D. willistoni	61	4–741	6	caf060213
D. mojavensis	57	1–741	6	caf051209
D. virilis	57	4–741	4	caf051209
D. grimshawii	57	1–741	6	caf051209
A. gambiae	51	22–639	10	ENSANG00000014371
A. aegyptus	49	18–647	10	EAT36134
T. castaneum	36	5–539	9	XP_969045

Orthologs of PFE in Drosophilid species, mosquito species and the red flour beetle. Single-pass transmembrane domains are predicted for all proteins listed and, with the exception of *A. gambiae*, all have predicted signal peptides. % identity and span (regions of shared identity) are based on BLAST 2 sequence output comparing protein x and PFE and #LRRs is the number of Leucine rich repeats predicted by SMART. See Experimental Procedures for details of bioinformatics.

Table 2

Real time PCR analysis of *PFE* in rdo^2

Drosophila Strain	Biological Samples	Transcripts (Fold-Change)	P (ANOVA)	Ct (*Gapdh2*)	Ct (*PFE*)
w^{1118}	3	1.0		15.57 ± 0.29	25.37 ± 1.23
rdo^2	3	-1.741 ± 0.37	0.1686	15.72 ± 0.24	27.11 ± 0.86

The level of wild-type (w^{1118}) transcript is defined as 1.0. Data (Mean ± SD) are fold-change in level of *PFE* transcript. '-' indicates a reduction in amount of *PFE* transcript relative to control (no significant difference). Data are normalized based on difference in average cycle threshold (Ct) for *Gapdh2* and *PFE*.